Video Article

Failure Analysis of Batteries Using Synchrotron-based Hard X-ray Microtomography

Katherine J. Harry[1,2], Dilworth Y. Parkinson[3], Nitash P. Balsara[2,4,5]

[1]Department of Materials Science and Engineering, University of California Berkeley

[2]Materials Science Division, Lawrence Berkeley National Laboratory

[3]Advanced Light Source Division, Lawrence Berkeley National Laboratory

[4]Department of Chemical and Biomolecular Engineering, University of California Berkeley

[5]Environmental Energy Technology Division, Lawrence Berkeley National Laboratory

Correspondence to: Katherine J. Harry at kharry@berkeley.edu

URL: https://www.jove.com/video/53021
DOI: doi:10.3791/53021

Keywords: Engineering, Issue 102, Lithium-ion batteries, lithium dendrite growth, polymer electrolytes, X-ray microtomography, electrochemistry, X-ray imaging

Date Published: 8/26/2015

Citation: Harry, K.J., Parkinson, D.Y., Balsara, N.P. Failure Analysis of Batteries Using Synchrotron-based Hard X-ray Microtomography. *J. Vis. Exp.* (102), e53021, doi:10.3791/53021 (2015).

Abstract

Imaging morphological changes that occur during the lifetime of rechargeable batteries is necessary to understand how these devices fail. Since the advent of lithium-ion batteries, researchers have known that the lithium metal anode has the highest theoretical energy density of any anode material. However, rechargeable batteries containing a lithium metal anode are not widely used in consumer products because the growth of lithium dendrites from the anode upon charging of the battery causes premature cell failure by short circuit. Lithium dendrites can also form in commercial lithium-ion batteries with graphite anodes if they are improperly charged. We demonstrate that lithium dendrite growth can be studied using synchrotron-based hard X-ray microtomography. This non-destructive imaging technique allows researchers to study the growth of lithium dendrites, in addition to other morphological changes inside batteries, and subsequently develop methods to extend battery life.

Video Link

The video component of this article can be found at https://www.jove.com/video/53021/

Introduction

Researchers are actively investigating battery chemistries with theoretical energy densities over an order of magnitude larger than traditional lithium-ion batteries.[1,2] These high-energy-density batteries will make electric vehicles more competitive with their gasoline-powered counterparts.[3] However, these new chemistries have several failure modes that preclude their use in commercial technologies. For example, these battery chemistries require a lithium metal anode to achieve large enhancements in energy density; unfortunately, lithium metal is prone to dendrite growth as lithium ions are reduced at the anode surface during charging.[4-9] Additionally, breakage of active particles in the cathode and poor adhesion within the battery can cause cell failure.[10]

Many modes of battery failure occur on the micrometer scale. However, most battery materials are air sensitive making sample preparation for analysis by electron microscopy and traditional optical microscopy difficult. Synchrotron hard X-ray microtomography allows one to visualize the interior of a battery without disassembly.[11-14] Furthermore, the technique produces a three-dimensional (3D) reconstruction of the assembled cell making it easy to find locations of failure.[15] Finding robust techniques that enable researchers to develop the scientific understanding required to accurately predict the lifetime of a battery is critical for the design of next generation battery technologies. The procedure discussed herein will specifically demonstrate how one can prepare and image model batteries to study the growth of lithium metal dendrites through solid polymer electrolyte membranes.

Computed tomography (CT) scanning is not a new technique and has been used frequently for failure analysis in industry. Synchrotron-based X-ray microtomography is advantageous because the high brightness and flux of the source allow collection of images with high resolution and good signal to noise in a much shorter amount of time.[16] Additionally, one can take advantage of the X-ray energy resolution to image at energies around a chemical species' absorption edge, causing the components containing that chemical species to be identified.[17] It was found that the synchrotron source provides sufficient flux to achieve good contrast between lithium metal and solid polymer electrolyte membranes enabling one to image lithium metal dendrites.[15]

The study discussed herein uses a high modulus, block copolymer electrolyte membrane.[18] These high modulus membranes suppress lithium dendrite growth, lengthening the lifetime of batteries.[19,20] However, dendrites still eventually puncture the membrane causing the battery to fail by short-circuit. It is important to understand the nature of dendrite formation and growth in these high modulus electrolyte membranes in order to design strategies to prevent their growth.

Protocol

1. Electrolyte Preparation

1. Synthesize a 240 kg/mol – 260 kg/mol poly(styrene) - *block* - poly(ethylene oxide) copolymer (SEO) using anionic polymerization.
    1. Perform all additional sample preparation in an Argon glovebox where the water and oxygen levels are controlled and remain <5 ppm.
    2. Dissolve 0.3 g of polymer in anhydrous N-methyl-2-pyrrolidone (NMP) with dry lithium bis(trifluoromethane)sulfonimide (LiTFSI) salt. Use a LiTFSI salt to SEO mass ratio of 0.275 and an NMP to SEO mass ratio of 13.13.
    Note: This quantity of polymer will yield a membrane large enough to make approximately 20 samples.
    3. Cast all of the polymer and salt mixture prepared in the steps above onto an approximately 15 cm by 15 cm square piece of nickel foil using a doctor blade. Dry the resulting film at 60 °C O/N.
    4. After drying, peel the film from the Nickel foil and allow to dry further under vacuum at 90 °C.
    5. Wrap the resulting freestanding film in Nickel foil and store inside an air-tight box in the glovebox for later use.

2. Lithium – Lithium Symmetric Cell Preparation

1. Use a 7/16 in diameter, round metal punch to cut out two lithium metal electrodes from a roll of 99.9% pure, battery-grade lithium metal foil.
2. Use a 1/2 in diameter metal punch to cut out a piece of polymer electrolyte film.
Note: The lithium metal is softer and easier to punch than the polymer electrolyte.
3. Sandwich the polymer electrolyte film between the two lithium metal electrodes and press the nickel tabs onto the electrodes.
4. Vacuum seal the sample in an air-tight pouch made of polypropylene and nylon lined aluminum.
Note: One of the lithium electrodes is easily swapped with a cathode if one wants to study a full battery.

3. Symmetric Cell Cycling

1. Place the vacuum-sealed sample into an oven held at 90 °C and cycle using electrochemical cycling equipment. Heat the sample during cycling to achieve reasonable ionic conductivity through the electrolyte membrane. For safety, ensure that the sample does not approach the lithium metal melting point of 180 °C.
2. Pass a current density of 0.175 mA/cm^2 through the sample for 4 hr and follow with a 45 min rest. Next, pass a current density of -0.175 mA/cm^2 through the sample for 4 hr and follow with a 45 min rest. Repeat this cycling routine as many times as desired.
3. Observe the voltage response for this current density passed through a 30 µm thick SEO electrolyte and compare with that shown in **Figure 1**. Stop the cycling routine when the cell voltage response drops to 0.00 V, because the battery has failed by short-circuit indicating the growth of lithium dendrites.

4. Synchrotron Hard X-ray Microtomography Imaging

1. After the symmetric cell is cycled, bring it back into the glove box and remove it from its pouch.
2. Use a 1/8 inch metal punch to cut out the center portion of the cell.Vacuum seal the center portion of the cell in pouch material and remove from the glovebox for transport to the synchrotron facility.
Note: By imaging a sample with a reduced diameter, the amount of material outside of the field of view of the X-ray detector is reduced. This improves the overall image quality by reducing noise caused by this extra material. Furthermore, removal of the highly X-ray absorptive Nickel current collectors is necessary, for this particular pouch design, to obtain clear X-ray images.
3. Once at the beamline, use polyimide tape to affix the sample to the sample stage. If desired, tape a small metal marker on top of the sample to aid with alignment. Place the metal marker roughly in the center of the sample to mark the location around which the sample will rotate once aligned.
4. Use 20 keV X-rays to image the sample with an exposure time optimized for the system. Optimize the exposure time by balancing the scan time and the number of counts per image. Estimate the total scan time by multiplying the exposure time by the number of images collected.
    1. Here, use an exposure time of 300 msec, resulting in a scan time of 5 to 10 min.
5. Measure the pixel size associated with the optical lenses at the beginning of every beamtime shift.
Note: For the 4x lens used to take the image shown in **Figure 2**, the pixel size was 1.61 µm/pixel. Higher magnification lenses (10x and 20x) are also available for use.
6. Position and align the sample on a rotation stage with respect to the detection system so that it remains in the detector's field of view as it rotates through 180°.
7. Position the sample as close to the detector as is possible while ensuring that the sample does not hit the detector at any rotation angle.
Note: As the sample to detector distance increases, the Fresnel phase contrast will become more pronounced in the reconstructed images. This can obscure features and result in poorer resolution. For pouch cells, the sample to detector distance is typically on the order of 3 cm away from the detector.
8. Once aligned, perform a scan consisting of 1,025 images collected over sample rotations between 0 and 180°. Collect "Bright field" (also known as "flat field" or "background") images by moving the sample out of the field of view. Additionally, collect "dark field" images by taking images while the beam is off. Use these to normalize the sample images for inhomogeneous illumination, scintillator response, and CCD camera response.

5. Image Reconstruction

1. Tomographically reconstruct the set of 1,025 radiographs into a stack of images where each image represents a slice in the volume using the following procedure.
    1. First, normalize the images by subtracting the “dark field” images from both the radiograph images and the “bright field” images. Divide the resulting radiograph images divided by the resulting “bright field” images.
    2. Next, perform tomographic reconstruction, the process by which the series of projection angles is transformed into a 3D image, on the normalized radiograph images according to manufacturer’s protocol.
    Note: The reconstruction software outputs a series of images, each representing a horizontal slice through the sample.When stacked, this set of reconstructed images form a three-dimensional X-ray absorption map of the sample.
2. Visualize the individual slices or the sample in three-dimensions to see what the sample looks like on the inside.

6. Data Visualization and Processing

1. Use one of a multitude of commercial and open source image processing software packages available for data visualization and analysis.[22, 23]
2. Upon opening the stack of reconstructed images with the desired software, create orthoslices to show the xy, xz, and yz perspectives of the reconstructed data.
3. Pan through these images and search for features of interest, like the lithium dendrite shown in **Figure 2**.
4. Next, use segmentation (digital labeling) and 3D rendering tools to render the feature of interest in three-dimensions.
5. To digitally segment the image, create a label field and use thresholding tools to select regions of the sample corresponding to a material.
6. To recreate an image like that shown in **Figure 2B**, label the dark pixels lithium and the bright pixels electrolyte. Label the lithium contained in the dendrite separately from the top and bottom lithium electrodes.
    1. Render the dendritic lithium in orange and the polymer electrolyte in blue. Render the top and bottom lithium metal electrodes in gray and adjust the transparency value to reveal the orange dendritic lithium. Rotate this three-dimensional reconstruction to view the structure from many perspectives.

Representative Results

When the symmetric lithium-lithium cells described above are cycled at 90 °C, the voltage response looks like that shown in **Figure 1**. Eventually, lithium dendrites will grow through the electrolyte and cause the cell to fail by short circuit. When this happens, the voltage response to the applied current will drop down to 0.00 V. Dendrites, like the one shown in **Figure 2** appear in samples that have failed by short circuit. Non-electrolyte spanning dendrites are also found in the samples. Using this method, one can study the evolution of dendrite growth as a function of the cell’s stage of life by imaging a series of samples cycled to various stages of life as discussed in reference 15. The dendrite morphology and size can be easily measured from the three-dimensional reconstructed images. Additionally, this technique allows the user to see structures that lie inside of the lithium metal electrode. These features are hidden when one uses other imaging techniques, like scanning electron microscopy or traditional optical microscopy.

Typical microtomography images taken of a symmetric lithium-lithium sample with a solid polymer electrolyte membrane and a schematic of the instrument used to obtain the data are shown in **Figure 2**. An example of a radiograph image is shown in **Figure 2A**. Once a series of radiographs are collected from many angles, the radiographs are reconstructed into a stack of image files. These reconstructed image files are cross-sectional slices through the sample and can be viewed with open source software like ImageJ,[23] or commercial software like Avizo.[22]**Figure 2B** shows an example of a cross-sectional slice taken from the stack of reconstructed images. This symmetric cell was cycled until it failed by electronic short-circuit. From the reconstructed images, it is apparent that the majority of the lithium metal electrode interface is featureless. However, one finds globular lithium dendrites extending through the solid polymer electrolyte membrane like that shown in the 3D rendering in **Figure 2C**. The globular features in the polymer electrolyte in **Figure 2C** are shrouded by the electrolyte itself. In contrast, the uniform character of the globular dendrite is clearly seen in the cross-section (**Figure 2B**). It is, perhaps, interesting to note that the radiograph image in **Figure 2A** has much less noise than the reconstructed slice shown in **Figure 2B**. The main advantage of the reconstruction is the clarity with which the dendritic structure can be seen; the dendritic structure cannot be discerned in **Figure 2A**.

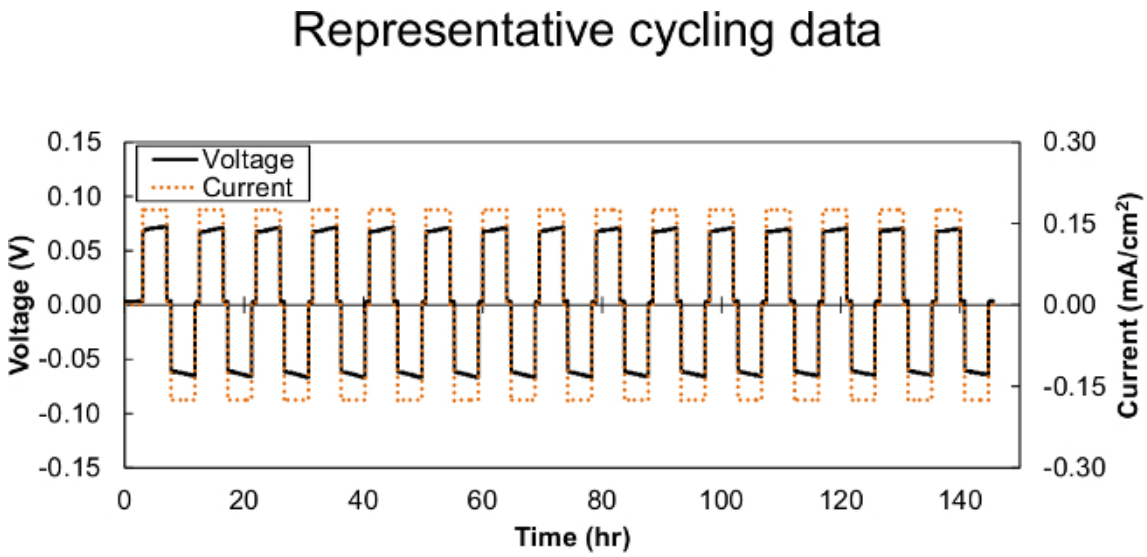

Figure 1. Chronopotentiometry. Representative cycling data for a lithium metal symmetric cell with a solid polymer electrolyte is shown. When a current density of 0.175 mA/cm^2 is applied to the cell, it responds with a voltage around 0.07 V. An alternating positive and negative current is applied to the cell to simulate the conditions of a battery charging and discharging. The sample rests for 45 min between each 4 hr charge and discharge. Please click here to view a larger version of this figure.

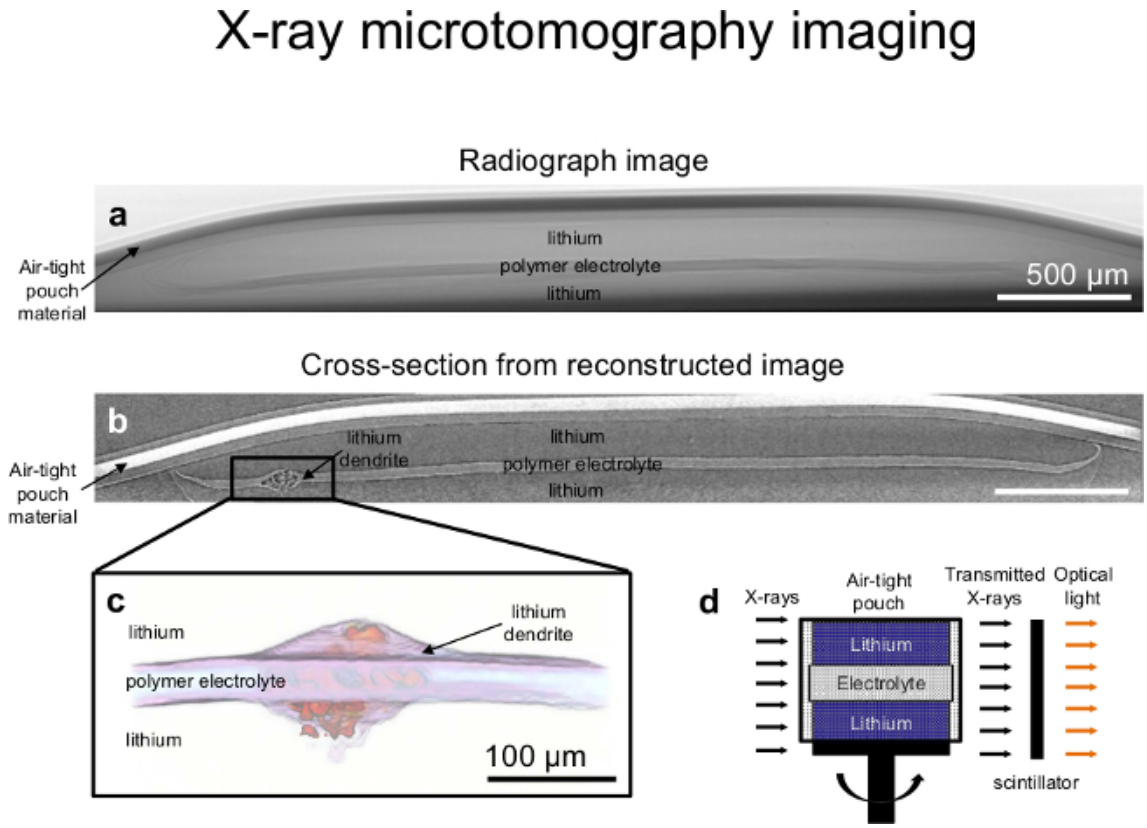

Figure 2. X-ray microtomography. Synchrotron hard X-ray microtomography is used to image a symmetric lithium cell that was cycled and failed by short circuit. **(A)** A radiograph image of the sample shows a dark polymer electrolyte band sandwiched between two lithium metal electrodes. The pouch material also appears in the image. **(B)** A cross-section slice through the reconstructed tomogram containing a lithium dendrite is shown. After reconstruction, the polymer electrolyte appears as a bright band sandwiched between two dark lithium metal electrodes. The pouch material also appears in the image. **(C)** Image segmentation was used to make a three-dimensional rendering of features in the sample. The dark, globular lithium metal dendrite is rendered in orange, so that the viewer can see its structure, while the bright, polymer electrolyte is rendered in purple. The top and bottom lithium metal electrodes are rendered transparent so they do not obscure the polymer electrolyte and the dendrite. **(D)** A schematic of the sample setup for X-ray microtomography experiments is shown. Please click here to view a larger version of this figure.

Discussion

Hard X-ray microtomography is especially well-suited for air-sensitive samples, like many electrochemically active materials, since the X-rays can penetrate through protective pouch material, enabling facile imaging of the sample without exposure to air. Perhaps the most valuable characteristic of this imaging technique is that the penetrating X-rays allow the user to see inside of the sample without destroying it. Most common imaging techniques, like scanning electron microscopy and traditional optical microscopy, can only image the surface of the electrodes. As such, many morphological changes that occur beneath the surface are hidden. X-ray imaging, however, allows the user to easily monitor the sample interior.

The theoretical resolution of this technique is less than a micrometer, but practical resolution is limited by absorption contrast and image noise. Also, the distance between the imaged region of the sample and the detection system impacts the resolution. Depending on the size of the pouch, the detection system is often 1-5 cm away from the central portion of the pouch, which contains the imaged material. This distance limits the resolution of the scan, both due to the rise of phase contrast artifacts with increasing distance, but also due to geometric blurring. Furthermore, the pixel size, determined by the magnification of the lens, will clearly influence the achievable resolution. X-ray absorption is a function of the atomic scattering factor, incident beam wavelength, and sample dimensions.[24] Roughly speaking, in the hard X-ray regime, the larger the atom, the more X-ray absorption occurs. Therefore, when imaging lithium dendrites, one can differentiate between lithium metal and the polymer electrolyte because the carbon-based electrolyte is more X-ray absorptive than lithium metal. Next, one must consider image noise. If the sample contains components made of large atoms, like nickel, a high percentage of the 20 keV X-rays will be absorbed by those components. If the majority of the X-rays are absorbed by these heavy components, the contrast between components made of lighter elements, like carbon and lithium, becomes negligible. We thus removed the nickel tabs from the cell before imaging.

The most critical step of the protocol is ensuring that the sample is designed in such a way that heavy metals like Nickel do not block the beam trajectory during imaging. The protocol described above is for *ex situ* imaging, and while less destructive than TEM or SEM imaging, still requires the sample to be destroyed. Efforts to create samples for *in situ* imaging by altering the position of the current collectors so that they do not block the path of the beam are currently underway.

To conclude, X-ray microtomography is a valuable tool for studying morphological changes in electrochemically active systems. Since the image resolution is limited to the micrometer scale, complementary experiments using traditional electron microscopy can help to clarify morphological changes on smaller length scales. Furthermore, some spectroscopic information can be obtained from this technique by taking images above and below the absorption edge of the element to be identified. Components in the sample containing that element will show a large change in contrast when the images are compared. However, this only works if the experimenter knows what element they wish to identify. Therefore, complementary spectroscopic techniques like Energy-dispersive X-ray spectroscopy would be necessary to identify unknown components in a sample. Using this tool, we were able to study the formation and growth of lithium dendrites through high modulus polymer electrolyte membranes.[15] We expect that the technique can be extended to study many micron-scale morphological changes that may occur upon cycling an electrochemical cell.

Disclosures

The authors have nothing to disclose.

Acknowledgements

Primary funding for the work was provided by the Electron Microscopy of Soft Matter Program from the Office of Science, Office of Basic Energy Sciences, Materials Sciences and Engineering Division of the U.S. Department of Energy under Contract No. DE-AC02-05CH11231. The battery assembly portion of the project was supported by the BATT program from the Vehicle Technologies program, through the Office of Energy Efficiency and Renewable Energy under U.S. DOE Contract DE-AC02-05CH11231. Hard X-ray microtomography experiments were performed at the Advanced Light Source which is supported by the Director, Office of Science, Office of Basic Energy Sciences, of the U.S. Department of Energy under Contract No. DE-AC02-05CH11231. Katherine J. Harry was supported by a National Science Foundation Graduate Research Fellowship.

References

1. Bruce, P. G., Freunberger, S. A., Hardwick, L. J., Tarascon, J. M. Li-O-2 and Li-S batteries with high energy storage. *Nat Mater.* **11**, 19-29 (2012).
2. Balsara, N. P., Newman, J. Comparing the Energy Content of Batteries, Fuels, and Materials. *J Chem Educ.* **90**, 446-452 (2013).
3. Girishkumar, G., McCloskey, B., Luntz, A. C., Swanson, S., Wilcke, W. Lithium - Air Battery: Promise and Challenges. *J Phys Chem Lett.* **1**, 2193-2203 (2010).
4. Selim, R., Bro, P. Some observations on rechargeable lithium electrodes in a propylene carbonate electrolyte. *J Electrochem Soc.* **121**, 1457-1459 (1974).
5. Aurbach, D., Zinigrad, E., Cohen, Y., Teller, H. A short review of failure mechanisms of lithium metal and lithiated graphite anodes in liquid electrolyte solutions. *Solid State Ionics.* **148**, 405-416 (2002).
6. Monroe, C., Newman, J. Dendrite Growth in Lithium/Polymer Systems. *J Electrochem Soc.* **150**, A1377 (2003).
7. Barton, J. L., Bockris, J. O. The Electrolytic Growth of Dendrites from Ionic Solutions. *Proc R Soc Ser A.* **268**, 485-505 (1962).
8. Bhattacharyya, R., *et al.* In situ NMR observation of the formation of metallic lithium microstructures in lithium batteries. *Nat Mater.* **9**, 504-510 (2010).
9. Chandrashekar, S., *et al.* 7Li MRI of Li batteries reveals location of microstructural lithium. *Nat Mater.* **11**, 311-315 (2012).

10. Arora, P., White, R. E., Doyle, M. Capacity fade mechanisms and side reactions in lithium-ion batteries. *J Electrochem Soc.* **145**, 3647-3667 (1998).
11. Ebner, M., Marone, F., Stampanoni, M., Wood, V. Visualization and Quantification of Electrochemical and Mechanical Degradation in Li Ion Batteries. *Science.* **342**, 716-720 (2013).
12. Qi, Y., Harris, S. J. In Situ Observation of Strains during Lithiation of a Graphite Electrode. *J Electrochem Soc.* **157**, A741-A747 (2010).
13. Eastwood, D. S., *et al.* Three-dimensional characterization of electrodeposited lithium microstructures using synchrotron X-ray phase contrast imaging. *Chem Commun.* (2014).
14. Shui, J. -L., *et al.* Reversibility of anodic lithium in rechargeable lithium–oxygen batteries. *Nat commun.* **4**, (2013).
15. Harry, K. J., Hallinan, D. T., Parkinson, D. Y., MacDowell, A. A., Balsara, N. P. Detection of subsurface structures underneath dendrites formed on cycled lithium metal electrodes. *Nat Mater.* **13**, 69-73 (2014).
16. Baruchel, J., *et al.* Advances in synchrotron hard X-ray based imaging. *Cr Phys.* **9**, 624-641 (2008).
17. Flannery, B. P., Deckman, H. W., Roberge, W. G., D'Amico, K. L. Three-Dimensional X-ray Microtomography. *Science.* **237**, 1439-1444 (1987).
18. Singh, M., *et al.* Effect of molecular weight on the mechanical and electrical properties of block copolymer electrolytes. *Macromolecules.* **40**, 4578-4585 (2007).
19. Monroe, C., Newman, J. The Impact of Elastic Deformation on Deposition Kinetics at Lithium/Polymer Interfaces. *J Electrochem Soc.* **152**, A396-1149 (2005).
20. Stone, G. M., *et al.* Resolution of the Modulus versus Adhesion Dilemma in Solid Polymer Electrolytes for Rechargeable Lithium Metal Batteries. *J Electrochem Soc.* **159**, A222-A227 (2012).
21. Panday, A., *et al.* Effect of Molecular Weight and Salt Concentration on Conductivity of Block Copolymer Electrolytes. *Macromolecules.* **42**, 4632-4637 (2009).
22. *Avizo v.8.1.* FEI Company Hillsboro, Oregon Available from: http://www.vsg3d.com/ (2014).
23. Schneider, C. A., Rasband, W. S., Eliceiri, K. W. NIH Image to ImageJ: 25 years of image analysis. *Nat methods.* **9**, 671-675 (2012).
24. Henke, B. L., Gullikson, E. M., Davis, J. C. X-Ray Interactions - Photoabsorption, Scattering, Transmission and Reflection at E=50-30,000 Ev, Z=1-92 (Vol 54, Pg 181, 1993). *Atom Data Nucl Data.* **55**, 349-349 (1993).

